MICROBIOLOGICAL METHODS

A Highly Sensitive Oligonucleotide Hybridization Assay for *Klebsiella pneumoniae* Carbapenemase with the Probes on a Gold Nanoparticles Modified Glassy Carbon Electrode

HONG-ZHI PAN[1]
Public Health School, Harbin Medical University, No. 157 Baojian Rd, Nangang District, Harbin, Heilongjiang Province, 150081, People's Republic of China
HONG-WEI YU,[1] **NA WANG, ZE ZHANG, GUANG-CAI WAN, HAO LIU, XUE GUAN, and DONG CHANG**[2]
The First Affiliated Hospital of the Harbin Medical University, No. 23 Youzheng St, Harbin, Heilongjiang Province, 150001, People's Republic of China

To develop a new electrochemical DNA biosensor for determination of *Klebsiella pneumoniae* carbapenemase, a highly sensitive and selective electrochemical biosensor for DNA detection was constructed based on a glassy carbon electrode (GCE) modified with gold nanoparticles (Au-nano). The Au-nano/GCE was characterized by scanning electromicroscopy, cyclic voltammetry, and electrochemical impedance spectroscopy. The hybridization detection was measured by differential pulse voltammetry using methylene blue as the hybridization indicator. The dynamic range of detection of the sensor for the target DNA sequences was from 1×10^{-11} to 1×10^{-8} M, with an LOD of 1×10^{-12} M. The DNA biosensor had excellent specificity for distinguishing complementary DNA sequence in the presence of non-complementary and mismatched DNA sequence. The Au-nano/GCE showed significant improvement in electrochemical characteristics, and this biosensor was successfully applied for determination of *K. pneumoniae*.

In recent years, extended-spectrum resistant bacteria pose a serious threat to human health. Drug-resistant bacteria infection lacks effective antibiotics, causing invalid treatment and aggravated infection even leading to death. That greatly increases the burden of individuals and families. Carbapenem resistance among *Klebsiella pneumoniae* is an emerging problem worldwide. Since *K. pneumoniae* carbapenemase (KPC) was first found in America (1), *K. pneumoniae* carbapenemase has spread rapidly around the world, and carbapenem resistance is becoming a major threat (2–5). The detection of KPC should be taken seriously in a clinicak laboratory, and the prevalence and outbreak of related hospital infection should also be prevented and controlled. Various culture-based methods (modified Hodge test and susceptibility testing) are often time-consuming and yield results only after additional cultivation for 24 or even 48 h (6). Automated susceptibility testing systems may fail to detect KPC-mediated resistance in clinical isolates (7); molecular diagnostic techniques such as real-time PCR have been shown to be sensitive and accurate methods for identifying the presence of carbapenemase genes (8, 9). This study is aimed to detect KPC and provide the basis for the rational use of antibiotics in clinics.

DNA biosensors are important in diagnostic tests for early cancer detection and identifying pathogens in products of food industries, forensic investigation, and assessment of medical treatment. Consequently, a wide variety of DNA biosensors based on different detection techniques has been developed. Among these techniques, electrochemical DNA biosensors are particularly attractive because of their low cost, high sensitivity, and portability (10). Especially, gold nanoparticles (Au-nano) have been used in biological detection and analysis due to their superior conductivity, huge surface area, and excellent catalytic action that produce electrochemical DNA biosensors characterized by rapidity, simplicity, and higher sensitivity (11–13). We developed an improved Au-nano/glassy carbon electrode (GCE) electrochemical DNA biosensor with methylene blue (MB) used as the hybridization indicator that can be applied to the detection of KPC. The electrochemical signal was detected by differential pulse voltammetry (DPV) and showed good linear relationship with complementary DNA sequence.

Experimental

Apparatus

Cyclic voltammetry (CV) and electrochemical impedance spectroscopy (EIS) were performed with a Model CHI660A electrochemical workstation (Shanghai Chenhua Instruments Co., Shanghai, China). Electrochemical measurements were performed using a three-electrode system consisting of an Ag/AgCL reference electrode (the concentration of KCl was 3 M), a platinum wire auxiliary electrode, and a modified GCE (3 mm diameter; all from Incole Union Technology Co. Ltd, Tianjin, China). Scanning electron microscopy (SEM) images were obtained using an FEI Sirion 2000 scanning electron microscope. Solution pH was measured with a pH

Received April 27, 2015. Accepted by AH June 15, 2015
[1] Author's contributed equally to this work.
[2] Corresponding author's e-mail: dongchang1969@163.com
DOI: 10.5740/jaoacint.15-105
Sources of support: This study was supported by grant 81273129 of the National Natural Science Fund of China.

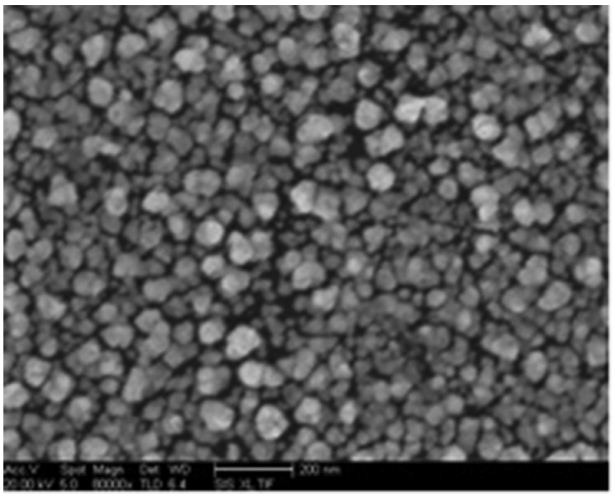

Figure 1. Images of Au-nano modified on GCE.

meter (Leici Instruments Co., Shanghai, China). The ultrasonic cleaning machine was from Kunshang Co., Ltd, JiangSu, China.

Reagents

MB and $HAuCL_4{\cdot}4H_2O$ were purchased from Sigma-Aldrich (St. Louis, MO). Potassium ferricyanide [$K_3Fe(CN)_6$] was purchased from Fuchen Chemical Reagent Co. (Tianjin, China). The buffers involved in this work were as follows: 0.1 M phosphate buffer solution (PBS; pH 7.0); 0.5% sodium dodecyl sulfate (SDS) solution; saline-sodium citrate buffer (2 × SSC) containing 300 mmol/L NaCl and 30 mmol/L $Na_3C_6H_5O_7$, which were purchased from GuangFu Technology Co. Ltd (Tianjin, China); and TE buffer solution containing 10 mmol/L Tris-HCl and 1 mmol/L $EDTANa_2$ (pH 8.0). All chemicals were analytical grade. Deionized water purified with a Millipore system (Millipore Ltd, Shanghai, China) was used throughout this study.

The following DNA sequences were studied:

Oligonucleotide sequence (ssDNA): SH-$(CH_2)_6$-5'-TCT GGA CCG CTG GGA GCT GG-3' was used as probe; complementary sequence: 5'-CCA GCT CCC AGC GGT CCA GA-3'; one-base mismatched sequence: 5'-CCA GCT CCC ATC GGT CCA GA-3'; three-base mismatched sequence: 5'-CTA GCT CCC ATC GGT CCA TA-3'; and non-complementary sequence: 5'-TTC ATG TTT CAT AAG TTG AG-3'.

All stock solutions were prepared in deionized water. At the same time, all oligonucleotides were dissolved in 10 mM Tris-HCl+1mM EDTA (TE buffer, pH 8.00). The synthetic oligonucleotides were purchased from Sangon Biotech Co. Ltd (Shanghai, China). Stock solution of probe DNA was prepared in TE buffer solution; other oligonucleotides were prepared in 2×SSC buffer solution.

Preparation of the GCE

Prior to modification, the bare GCE was polished to a mirror-like surface with 0.05 μm and 1 μm alumina slurry on micro-cloth pads. The electrode was then rinsed thoroughly with ultrapure water and cleaned ultrasonically and sequentially in ultrapure water, absolute ethanol, and acetone for 3 min. Finally the bare electrodes were scanned in 0.2 M KNO_3 and 1 mmol/L $K_3Fe(CN)_6$ between −0.1 and 0.6 V at a scan rate of 0.05 V/s until a reproducible potential difference less than 70 mv was obtained. All electrodes were washed with ultrapure water and dried in a nitrogen atmosphere until further use.

Au-nano/GCE

The pretreated GCE was dipped in 0.05 M H_2SO_4 mixed with 5×10^{-3} M $HAuCL_4$. Then Au-nano particles were fabricated on the GCE by potentiostatic deposition to acquire the Au-nano self-assembled GCE. After that, the Au-nano/GCE was activated by CV twice to stability from –0.2 to 1.6 V at 50 mv/s in 0.5 M H_2SO_4.

Immobilization of Probe DNA

Immobilization of the ssDNA was achieved by dropping 10 μL 1.0×10^{-6} ssDNA onto the surface of the Au-nano/GCE and drying naturally at room temperature. It was then rinsed with TE buffer and ultrapure water three times to remove unfixed ssDNA. The biosensor was obtained and denoted as ssDNA/Au-nano/GCE. Then it was stored in a refrigerator at 4°C.

Hybridization with Complementary DNA

The ssDNA/Au-nano/GCE was immersed into 2×SSC buffer solution containing complementary DNA for 30 min at 50°C. Then it was rinsed with 0.5% SDS and deionized water respectively to remove the unhybridized complementary DNA. The obtained electrode was denoted as dsDNA/Au-nano/GCE.

Electrochemical Detection of DNA Hybridization

The hybridization process was performed by immersing the ssDNA/Au-nano/GCE and dsDNA/Au-nano/GCE into MB PBS solution (0.1 M, pH 7.0) and then stirring gently for 20 min. After that, the modified electrodes were rinsed with deionized water. Finally the modified electrodes were scanned with DPV ranging from –0.6 to 0.2 V at 50 mv/s in PBS, using MB as an electrochemical indicator. In this study, variations of the oxidation peak current of MB were used to quantify the concentration of complementary DNA.

Results and Discussion

Characterization of Electrodes

(a) *Morphological characteristics of Au-nano/GCE.*—SEM was used to investigate the surface morphological characteristics of the Au-nano/GCE. Figure 1 shows that Au-nano particles with diameter between 50 and 70 nm have been equitably modified onto the GCE. The image indicates that this method can form an Au-nano self-assembled GCE.

(b) *Characterization of different electrodes.*—Figure 2 shows the CV behavior for four different modified electrodes in 1 mmol/L $[Fe(CN)_6]^{3-/4-}$ aqueous solution containing 0.2 M KNO_3 at a scan rate of 50 mV/s. Compared with bare electrode (B), the peak current at the Au-nano/GCE was increased and the peak potential was decreased, which indicated that Au-nano have excellent conductivity and catalysis. It is also

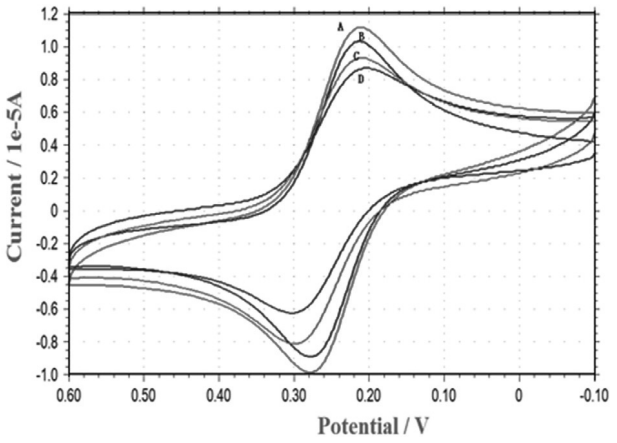

Figure 2. Cyclic voltammograms of different electrodes: (A) Au-nano/GCE; (B) bare electrode; (C) ssDNA/Au-nano/GCE; and (D) dsDNA/Au-nano/GCE.

shown in Figure 2 that ssDNA/Au-nano/GCE exhibited peak current reduction and peak potential increase, the probable reason being the electrostatic repulsion that occurred between negative-charged phosphate of ssDNA and $[Fe(CN)_6]^{3-/4-}$, which resist electron transfer. The reduction of the peak current was preceded by the hybridization of the probe DNA with the target DNA (D). This can attributed to increased negative charges on electrode surface after hybridization of the probe DNA with the target DNA, resulting in repulsion of $[Fe(CN)_6]^{3-/4-}$. Also, immobilization of the probe DNA and target DNA lead to increased density on the Au electrode surface and prevent electron transfer between the electrode surface and electroactive species.

EIS has been proven to be one of the most powerful tools for probing the features of surface-modified electrodes. Figure 3 shows the electron transfer resistance changes of Au-nano/GCE (A), ssDNA/Au-nano /GCE (B), dsDNA/Au-nano/GCE (C), and bare GCE (D). It can be seen that Au-nano/GCE (A) exhibited a relatively low impedance value in Figure 3 (A), which was characteristic of a diffusion-limiting step of the electrochemical process and assisted electron transfer. The charge transfer resistance values were determined directly from the diameters of the high frequency semicircle, with respect to the different electrodes. An apparent difference in the impedance spectra was observed; the diameter of the high frequency semicircle of ssDNA/Au-nano/GCE (B) and dsDNA/Au-nano/GCE (C) were almost reduced to about half of that for bare GCE. So we concluded that Au-nano caused the impedance value decrease and enhanced the conductivity of Au-nano/GCE. It also proved that dsDNA/Au-nano/GCE impedance value increased compared with ssDNA/Au-nano/GCE due to more negative charges on dsDNA.

Cyclic Voltammograms of MB on Different Electrodes

All four different electrodes were immersed in PBS solution fixed with MB, then scanned by CV in blank PBS solution. The results are shown in Figure 4; it can be seen that three obvious redox peaks of MB were observed with Au-nano/GCE (curve B), dsDNA/Au-nano/GCE (curve C), and ssDNA/Au-nano/GCE (curve D) but not the bare GCE. This demonstrates that MB was immobilized on Au-nano/GCE, dsDNA/Au-nano/GCE, and ssDNA/Au-nano/GCE in different density. Many free guanine bases of ssDNA were exposed and had a strong affinity for MB; hence, a large amount of MB accumulation occurred on the surface of ssDNA/Au-nano/GCE. Therefore, the highest MB oxidoreduction signal was observed with ssDNA probe on Au-nano/GCE. However, a significant decrease in voltammetric peak current of MB was observed after complementary DNA sequence was allowed to hybridize with Au-nano/GCE (curve C). The decline of current signal after hybridization was probably due to the inaccessibility of the guanine bases in dsDNA. The reason may be that there was no free guanine base exposed in dsDNA, so a different binding mode of MB with ssDNA/Au-nano/GCE and dsDNA/Au-nano/GCE resulted in variation in electrochemical responses. These results were consistent with a report in the literature (14).

Optimization of Experimental Conditions

(a) *Optimization of MB concentration.*—It is well known that the assay conditions affect the performance of a biosensor. Peak currents of ssDNA/Au-nano/GCE with varying MB concentrations from 1×10^{-6} to 1×10^{-4} M were observed; the current increased significantly with increasing MB concentration up to 2×10^{-5} M. When MB concentration continued to increase, the current increased slowly and finally flattened out. This result arose from MB aggregation on the surface of ssDNA/Au-nano/GCE.

(b) *Optimization of adsorption time.*—We investigated the effect of adsorption time on the response signal. ssDNA/Au-nano/GCE was immersed in 2×10^{-5} M MB solution and then scanned in PBS solution. It was observed that the response signal increased significantly with increasing adsorption times from 1 to 25 min. When the adsorption time exceeded 25 min, the response signal remained relatively constant, indicating that adsorption had reached saturation. Thus, 25 min adsorption time was selected in this study.

(c) *Optimization of hybridization temperature and time.*—The effect of temperature on the biosensor response was investigated; the peak current of MB increased significantly when the temperature changed from 25 to 50°C. At higher temperatures, the current response decreased slowly because of the denaturation of complementary DNA sequence. Then, the

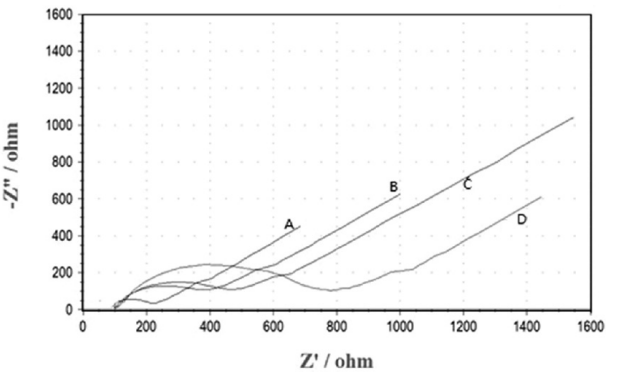

Figure 3. Nyquist diagram of different electrodes: (A) Au-nano/GCE; (B) ssDNA/Au-nano/GCE; (C) dsDNA/Au-nano/GCE; and (D) bare GCE.

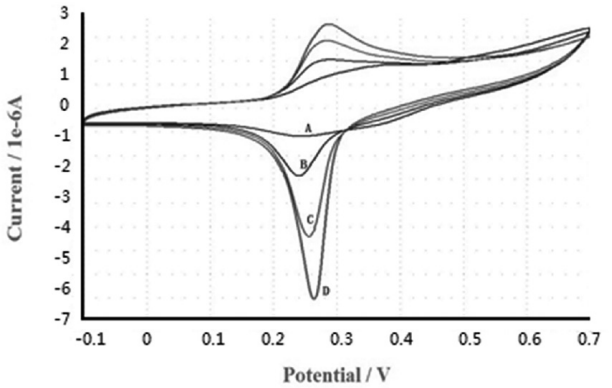

Figure 4. Cyclic voltammograms of different electrodes in MB solution: (A) bare GCE; (B) Au-nano/GCE; (C) dsDNA/Au-nano/GCE; and (D) ssDNA/Au-nano/GCE.

effect of DNA hybridization time on the peak current of MB was investigated. The designed biosensor exhibited a clearly increasing response with increasing hybridization times but remained stable after 60 min, indicating that the hybridization reaction was completed during 60 min. Thus, we chose the hybridization temperature of 50°C and the hybridization time of 60 min in subsequent experiments.

Performance Evaluation of the Electrochemical Biosensor

(a) *Analytical performance of the biosensor.*—Under optimal conditions, analytical performance of this electrochemical DNA biosensor was investigated by varying the complementary DNA concentration according to the procedures described above. As shown in Figure 5, the different current value obtained in the DPV response of MB after hybridization of ssDNA probe with complementary DNA sequence was recorded. The current response showed excellent correlation with the amount of complementary DNA sequence in the range from 1×10^{-11} to 1×10^{-8} M. The regression equation was $\Delta I = 2.0668 \log C + 25.197$ (unit of C is M, unit of I is μA), $R^2 = 0.9989$. The LOD was 1×10^{-12} M.

(b) *Selectivity of the electrochemical biosensor.*—The different DNA sequences at 1×10^{-8} M were detected by ssDNA/Au-nano/GCE. The signals are shown in Figure 6. It was indicated that this electrochemical DNA biosensor has excellent selectivity to complete complementary DNA sequence.

(c) *Reproducibility of the biosensor.*—Reproducibility of the response is an important characteristic for the modified electrode that should be explored for analytical determinations. Five different biosensors were fabricated independently under the same conditions and were then used to detect complementary DNA at 1×10^{-9} M according to the procedures described above. The RSD was 5.8%, indicating that the electrochemical DNA biosensor has excellent reproducibility.

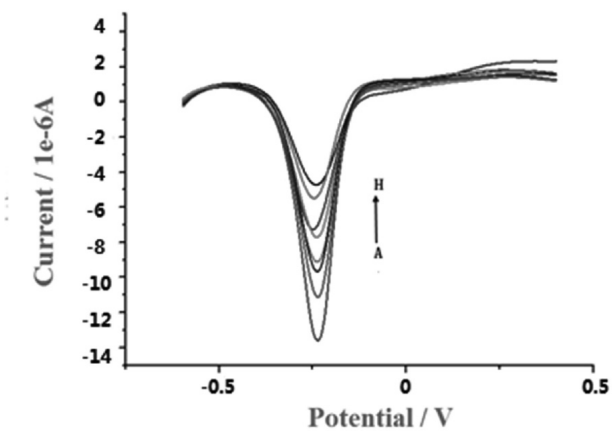

Figure 5. DPV curves of Au-nano/GCE hybridized with increasing concentrations of complementary DNA. A-H: 1×10^{-8} M, 5×10^{-9} M, 1×10^{-9} M, 5×10^{-10} M, 1×10^{-10} M, 5×10^{-11} M, 1×10^{-11} M, 5×10^{-12} M.

Conclusions

In this work, we have introduced a strategy for DNA hybridization detection by using an Au-nano/GCE. The electrochemical DNA biosensor showed high sensitivity, excellent selectivity, and good stability. It should be pointed out that the electrochemical DNA biosensor can effectively recognize the complementary DNA. It might have a promising future for detection of KPC and solve the problem of early diagnosis.

Acknowledgments

This study was supported by grant 81273129 of the National Natural Science Fund of China and YJSCX2015-53HYD of Harbin Medical University. The authors greatly appreciated this support.

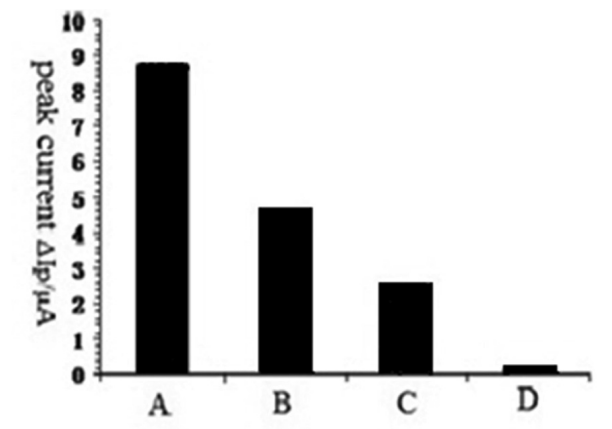

Figure 6. The peak current changes of the biosensor recognizing different target DNA: (A) complementary sequence; (B) one-base mismatched sequence; (C) three-base mismatched sequence; and (D) non-complementary sequence.

References

(1) Yigit, H., Queenan, A.M., Anderson, G.J., Domenech-Sanchez, A., Biddle, J.W., Steward, C.D., Alberti, S., Bush, K., & Tenover, F.C. (2001) *Antimicrob. Agents Chemother.* **45**, 1151–1161. http://dx.doi.org/10.1128/AAC.45.4.1151-1161.2001

(2) Tseng, S.P., Wang, J.T., Liang, C.Y., Lee, P.S., Chen, Y.C., & Lu, P.L. (2014) *Antimicrob. Agents Chemother.* **58**, 593–595. http://dx.doi.org/10.1128/AAC.00231-13

(3) Tsakris, A., Voulgari, E., Poulou, A., Kimouli, M., Pournaras, S., Ranellou, K., Kosmopoulou, O., & Petropoulou, D. (2010) *J. Clin. Microbiol*. **48**, 2546–2549. http://dx.doi.org/10.1128/JCM.00264-10

(4) Roche, C., Cotter, M., O'Connell, N., & Crowley, B. (2009) *Euro. Surveill.* **14**, pii:19163

(5) Rojas, L.J., Mojica, M.F., Blanco, V.M., Correa, A., Montealegre, M.C., De La Cadena, E., Maya, J.J., Camargo, R.D., Quinn, J.P., & Villegas, M.V. (2013) *Antimicrob. Agents Chemother.* **57**, 1101–1102. http://dx.doi.org/10.1128/AAC.01666-12

(6) Sun, K., Chen, X., Li, C., Yu, Z., Zhou, Q., & Yan, Y. (2015) *APMIS* **123**, 123–127. http://dx.doi.org/10.1111/apm.12313

(7) Anderson, K.F., Lonsway, D.R., Rasheed, J.K., Biddle, J., Jensen, B., McDougal, L.K., Carey, R.B., Thompson, A., Stocker, S., Limbago, B., & Patel, J.B. (2007) *J. Clin. Microbiol*. **45**, 2723–2725. http://dx.doi.org/10.1128/JCM.00015-07

(8) Nakano, R., Nakano, A., Ishii, Y., Ubagai, T., Kikuchi-Ueda, T., Kikuchi, H., Tansho-Nagakawa, S., Kamoshida, G., Mu, X., & Ono, Y. (2015) *J. Infect. Chemother.* **21**, 202–206. http://dx.doi.org/10.1016/j.jiac.2014.11.010

(9) Tuite, N., Reddington, K., Barry, T., Zumla, A., & Enne, V. (2014) *J. Antimicrob. Chemother.* **69**, 1729–1733. http://dx.doi.org/10.1093/jac/dku083

(10) Mascini, M., Palchetti, I., & Marrazza, G. (2001) *Fresen. J. Anal. Chem*. **369**, 15–22. http://dx.doi.org/10.1007/s002160000629

(11) Wipawakarn, P., Ju, H., & Wong, D.K.Y. (2012) *Anal. Bioanal. Chem.* **402**, 2817–2826. http://dx.doi.org/10.1007/s00216-012-5733-0

(12) Wang, M., Du, X., Liu, L., Sun, Q., & Jiang, X. (2008) *Chin. Anal. Chem.* **36**, 890–894. http://dx.doi.org/10.1016/S1872-2040(08)60048-1

(13) Lei, Y., Feng, M., Wang, K., Lin, L., Chen, Y., & Lin, X. (2013) *Anal. Bioanal. Chem.* **405**, 423–428. http://dx.doi.org/10.1007/s00216-012-6477-6

(14) Liu, Z., Liu, Y., Shen, G., & Yu, R. (2008) *Anal. Lett.* **41**, 1083–1095. http://dx.doi.org/10.1080/00032710801978608